Paper #33 GENETIC VARIATION OF PROPIONIBACTERIUM ACNES AND ASSOCIATION WITH ORTHOPEDIC SHOULDER INFECTIONS

K. Keely Boyle, MD, Scott R. Nodzo, MD, John K. Crane, MD, PhD, ***Thomas R. Duquin, MD,*** *Jacobs School of Medicine, University at Buffalo, Buffalo, New York, USA*

Introduction: *Propionibacterium acnes* (*P. acnes;* also referred to as *Cutibacterium acnes or C. acnes*) is the most commonly isolated organism during revision shoulder arthroplasty. Given the ubiquity of *C. acnes* as common skin flora, differentiating true infection from contamination remains a clinical diagnostic dilemma. Next generation sequencing, a molecular technique for identifying microbial profiles, found bacterial DNA in 25% of aseptic arthroplasty revisions with the most prevalent organism being *P. acnes*. *C. acnes* pathogenicity is associated with numerous virulence properties, including eliciting an enhanced host inflammatory response, biofilm formation, and antibiotic resistance. Beta-hemolytic activity expressed phenotypically as hemolysis has been shown to correlate clinically with true orthopedic shoulder infections, possibly serving as a marker for virulence. We sought to gain a greater understanding of the virulence properties of *C. acnes* through molecular analysis by comparing the gene expressions of previously determined clinically infected isolates versus isolates determined to be contaminants.

Methods: A retrospective review of 58 patients with a positive *C. acnes* culture(s) at time of revision surgery or during diagnostic aspiration of a shoulder arthroplasty was performed including demographics, preoperative and intraoperative findings, laboratory values, and clinical course. The periprosthetic shoulder infection criteria developed by Frangiamore et al. was used to classify patients into the following categories: *Definite Infection, Probable Infection*, and *Probable Contaminant.* Six *C. acnes* isolates from six patients were chosen for molecular analysis. Three isolates with a hemolytic phenotype were chosen from the *Definite Infection* group (D1-D3) and three isolates with a non-hemolytic phenotype from the *Probable Contaminant* group (C1-C3) for RNA sequencing (RNA-seq). The bacterial isolates were stored on CryoCare Beads at –70° C, grown on Brucella Blood agar plates using three-quadrant streaking and incubated at 37°C for 48 hours under anaerobic conditions using the GasPak EZ anaerobe pouch system. Total RNA was extracted from each isolate using Qiagen AllPrep DNA/RNA Purification Kit. Quality control was performed on all RNA extractions. RNA libraries were prepared using the TruSeq Stranded prep kit and sequenced on the Illumina NextSeq500. The RNA-seq data was analyzed using the R Bioconductor package DESeq2 to determine differential gene expression based on a model using the negative binomial distribution. Principal component and heatmap analysis was used to determine the variation and patterning between the *Definite Infection* and *Probable Contaminant* gene sequences.

Results: The three isolates classified as *Definite Infection* demonstrated similar gene expression with minimal variance between strains when compared to the *Probable Contaminants* (Fig. 1). Principal component analysis (PCA) was performed using the top 500 most variable genes. The first principle component (PC1) explained 49% of the variance in gene expression, and was able to discriminate between the *Definite Infections* (red), *Probable Contaminants* (blue) and additionally, *Probable Contaminant* sample C3 (Fig. 1). The second principle component (PC2) explained 38% of the variance and was able to discriminate between *Definite Infections* and *Probable Contaminants*. A heatmap of the sample-to-sample distances was used to visualize the similarities and dissimilarities between sample gene-expression (Fig. 2). The heatmap demonstrated similar gene expression in the three *Definite Infections*, and significantly different expression when compared to the *Probable Contaminant* isolates. The *Probable Contaminant* group had more genes that were highly differentially expressed, including hyaluronate lyase, which degrades hyaluronan and chondroitin. The *Definite Infection* isolates highly expressed genes representing ABC transporters, which

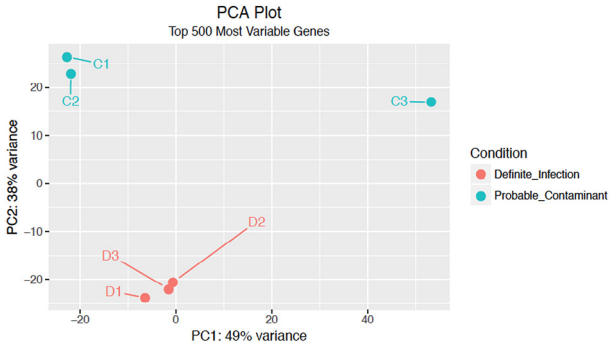

Figure 1 PCA Plot comparing variations in gene expression between strains classified as Definite Infection and Probable Contaminant.

are essential in cell viability, virulence, pathogenicity and antimicrobial resistance.

Discussion: Many surgeons continue to face the clinical dilemma associated with interpretation of a positive aspiration or an unexpected positive *C. acnes* culture in the setting of revision shoulder arthroplasty. The results of this study support a genetic difference between the strains causing definite clinical infections and probable contamination. Future research will be devoted to further understanding the clinical importance of the variance in gene expression and the relation to pathogenicity.

Conclusion: *C. acnes* revision TSA isolates classified as *Definite Infection* demonstrated a significant variance in gene expression

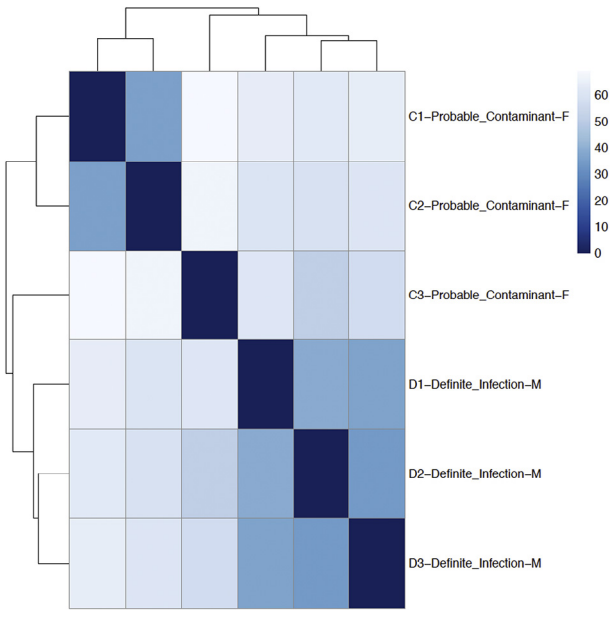

Figure 2 Heatmap: A heatmap visualizes the similarities and dissimilarities between sample gene-expression. The Definite Infection group show similarity to each other and dissimilarity to the Probable Contaminant group.

compared to isolates classified as *Probable Contaminants*, indicating distinct differences in those strains causing clinically relevant orthopedic shoulder arthroplasty infections.

Further reading

1. Higgins C. ABC transporters: physiology, structure and mechanism. Res Microbiol 2001;152:205-2010.
2. Love MI, Huber W, Anders S. Moderated estimation of fold change and dispersion for RNA-seq data with DESeq2. Genome Biol 2014;15:550. http://dx.doi.org/10.1186/s13059-014-0550-8
3. Tarabichi M, Shohat N, Goswami K, Alvand A, Silibovsky R, Belden K, et al. Diagnosis of periprosthetic joint infection: the potential of next-generation sequencing. J Bone Joint Surg Am 2018;100:147-54. http://dx.doi.org/10.2106/JBJS.17.00434

Paper #34 ANALYSIS OF HUMAN MUSCLES OF THE SHOULDER AND UPPER EXTREMITY A TEMPORAL PROFILE OF HUMAN MOTOR ENDPLATE DEGRADATION

Ranjan Gupta, MD[a], *Justin Chan, BA*[a], *Jennifer Uong*[a], *Winnie Palispis, MD*[a], *Oswald Steward, PhD*[a], *Thay Q. Lee, PhD*[b], [a]*Peripheral Nerve Research Lab, Department of Orthopaedic Surgery, University of California, Irvine, Irvine, California, USA;* [b]*Orthopaedic Biomechanics Lab, Long Beach VA Health System, Long Beach, California, USA*

Hypothesis: The suprascapular nerve is prone to traumatic injury during falls on an out-stretched hand, as well as secondary to blunt trauma to the top of the shoulder, due to its relatively fixed position under the ligaments and rotator cuff as well as high position on the brachial plexus. The supraspinatus muscle is innervated by the suprascapular nerve and routinely undergoes fatty degeneration and fibrosis with rotator cuff pathology in a manner that grossly seems analgous to a nerve injury. Although the supraspinatus is also the most studied muscle of rotator cuff, the pathophysiology of motor endplate degeneration specific to humans is not well understood. Patients with traumatic peripheral nerve injuries provide a unique opportunity to capture this invaluable data about human muscle degeneration.We hypothesized that the time course of human motor endplate degeneration after traumatic nerve injury is temporally correlated with the duration of denervation after traumatic nerve injury. We tested this hypothesis by rigorously analyzing denervated human muscle tissue to build a temporal profile of neuromuscular junction (NMJ) degeneration after a distinct, identifiable injury so as to better understand end stage human muscle degeneration.

Methods: IRB approval was obtained so as to permit biopsies from denervated muscles in patients with injuries ranging from complete pre-ganglionic C5-T1 brachial plexus injuries to less severe, but distinct, traumatic nerve injuries. Specimens were processed for immunohistochemistry and visualized with two-photon excitation and confocal microscopy. Human muscle samples from multiple timepoints after injury were analyzed along with control specimens from innervated muscles so as to create a temporal sequence of events for human motor endplate degradation following traumatic nerve injury.

Results: Denervated muscle samples show distinct differences from innervated muscles, including fragmentation and dispersion of acetylcholine receptors (Fig. 1). There is also a noted decrease in NMJ volume as seen in 3D reconstruction, and a trend towards plaque endplate morphology. Moreover, comparison of denervated muscles shows signs of temporal degeneration. NMJs from early denervated muscles still show well preserved circular morphology with definite acetylcholine receptors arranged in distinct folding patterns. By one year status post traumatic brachial injury, NMJs begin to present with greater fragmentation (Fig. 2). Moreover, synaptic gutters start to fade, and asymmetry in acetylcholine receptor distribution is noted. Interestingly, even after one year of denervation, NMJs were able to retain their overall circular shape.

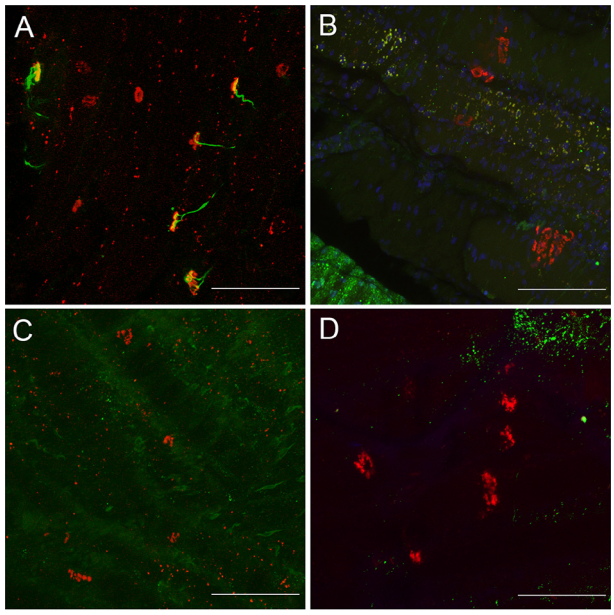

Figure 1 Confocal images of human NMJs. (A) innervated deltoid. (B) 5 month denervated first dorsal interossei. (C) 4 month denervated biceps. (D) 1 year denervated biceps. BTX = α-bungarotoxin. NF/syn = neurofilament and synaptophysin. Scale bars = 50 μm (20×).

Summary: This study details the novel and critically important data about the sequence of events involved in human motor endplate degradation after a clearly defined traumatic injury. Surprisingly, human NMJs persist and retain their structures even after the 6-month window of opportunity for meaningful functional recovery has elapsed. These findings may indicate a limited utility of animal models for traumatic peripheral nerve injuries and point to better understanding the morphometric changes in human muscle after injury.

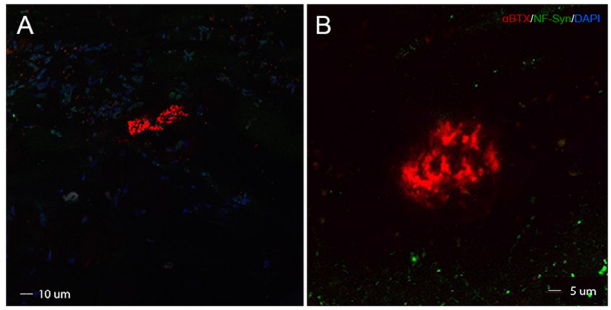

Figure 2 Staining of NMJs from biceps muscle one year after traumatic brachial plexus injury. (A) NMJ at low magnigication. (B) NMJ at higher magnification. Red for alpha-bungarotoxin, blue for DAPI, green for neurofilament and synaptophysin.